Published in final edited form as:
Nat Methods. 2011 March ; 8(3): 267–272. doi:10.1038/nmeth.1564.

Quantification of $PtdInsP_3$ molecular species in cells and tissues by mass spectrometry

Jonathan Clark[1,2,5], **Karen E. Anderson**[1,5], **Veronique Juvin**[1], **Trevor S. Smith**[1], **Fredrik Karpe**[3,4], **Michael J.O. Wakelam**[1], **Len R. Stephens**[1,5], and **Phillip T. Hawkins**[1,5]

[1]Inositide Laboratory, Babraham Institute, Babraham Research Campus, Cambridge, United Kingdom

[2]Babraham Bioscience Technologies Ltd., Babraham Research Campus, Babraham, Cambridge, United Kingdom

[3]Oxford Centre for Diabetes, Endocrinology and Metabolism, University of Oxford, Oxford, United Kingdom

[4]NIHR Oxford Biomedical Research Centre, ORH Trust, Churchill Hospital, United Kingdom

Abstract

Class I phosphoinositide-3-kinase (PI3K) isoforms generate the intracellular signalling lipid, phosphatidylinositol(3,4,5)trisphosphate (PtdIns(3,4,5)P_3). PtdIns(3,4,5)P_3 regulates major aspects of cellular behavior and the use of both genetic and pharmacological intervention has revealed important isoform-specific roles for PI3Ks in health and disease. Despite this interest, current methods for measuring PtdIns(3,4,5)P_3 have major limitations, including insensitivity, reliance on radiolabeling, low throughput and an inability to resolve different fatty-acyl species. We introduce a methodology based upon phosphate methylation coupled to high performance liquid chromatography-mass spectrometry (HPLC-MS) to solve many of these problems and describe an integrated approach to quantify PtdIns(3,4,5)P_3 and related phosphoinositides (regio-isomers of PtdInsP and PtdInsP_2 are not resolved). This methodology can quantify multiple fatty-acyl species of PtdIns(3,4,5)P_3 in un-stimulated murine and human cells (≥ 10^5) or tissues (≥ 0.1 mg) and their increase upon appropriate stimulation.

Introduction

PI3Ks phosphorylate one or more of the three canonical phosphoinositides that are found in all eukaryotic cells, PtdIns, PtdIns4P and PtdIns(4,5)P_2, to form PtdIns3P, PtdIns(3,4)P_2 and PtdIns(3,4,5)P_3, respectively. These lipid products are now recognized as pivotal intracellular signals that act by dictating the localization and activity of several key regulators of cellular function[1-2]. The Class I PI3Ks, of which there are four isoforms in mammalian cells (α, β, δ and γ), can be activated by many groups of cell surface receptors to accelerate production of PtdIns(3,4,5)P_3 in the inner leaflet of the plasma membrane. A

Correspondence to Phillip Hawkins/ Len Stephens; Inositide Laboratory, Babraham Institute, Babraham Research Campus, Cambridge CB2 4AT, UK. Phone: (44)-1223-496598; Fax: (44)-1223-496043; phillip.hawkins@bbsrc.ac.uk, len.stephens@bbsrc.ac.uk.
[5]KEA and JC contributed equally; LRS and PTH contributed equally.

Author Contributions:

JC and KEA designed and performed experiments, developed methods, analysed data, and contributed to writing the manuscript; VJ designed and performed PKB experiments; TSS performed experiments; FK designed experiments (Fig. 5, Supplementary Figs. S9-10) to generate samples for analysis; MJOW developed methods, and provided reagents; and LRS and PTH designed the study/ experiments, developed methods, analysed data and wrote the manuscript.

Europe PMC Funders Author Manuscripts

diverse family of proteins can selectively bind PtdIns(3,4,5)P_3 via their conserved PH domains, resulting in their activation and hence further translation and propagation of the original receptor signal.

Many cell processes are regulated by Class I PI3Ks, including growth, survival and movement. Remarkably, despite the fact they all make a common output signal, PtdIns(3,4,5)P_3, the different Class I PI3K isoforms perform different roles in both physiology and pathology[3]. This, combined with the drugability of their active sites, has led to substantial investment in targeting the Class I PI3Ks in a variety of disease settings such as PI3Kγ and PI3Kδ in inflammation and PI3Kα in oncology.

The amphiphilic phosphoinositides, including PtdIns(3,4,5)P_3, have been quantified by a number of methods. Broadly, these all show that the levels of PtdIns(3,4,5)P_3 in un-stimulated cells are “very low” (typically undetectable) and rise five to fifty fold on stimulation, to reach concentrations that are, at most, 10% of cellular PtdIns(4,5)P_2. These techniques have a variety of problems, including sensitivity, sample through-put, dynamic range and applicability across a range of sample formats[4-6]. Further, like all phospholipids, phosphoinositides contain a wide range of potential constituent fatty acid moieties and thus, in reality, comprise families of molecular species with a common headgroup. Classical chromatographic techniques and, more recently, mass-spectrometry-based lipidomics approaches have been developed that can resolve many families of fatty-acyl species, including those of the phosphoinositides[4,7-12]. PtdIns(3,4,5)P_3 however, has proven very difficult to quantify using these approaches, primarily due to problems with recovery, stability and yield of the relevant ions[7,9,13].

These issues have seriously hampered progress in understanding the Class I PI3K signaling pathway. In particular, the inability to quantify the pathway’s primary output signal is proving a major obstacle in developing an adequate, quantitative understanding of information flow through this pathway, including attempts to model the system. It has also hampered the development of biomarkers for reading out the impact of inhibitors of this pathway *in vivo*. This has lead to many workers using surrogate assays of pathway activity, such as phosphorylation levels of PKB, which are indirect and can be disconnected from PI3K signalling under some circumstances[14]. The inability to discriminate different fatty-acyl species of PtdIns(3,4,5)P_3 has also prevented any serious attempt to elucidate their functional significance.

We now present an integrated HPLC-MS based methodology that allows absolute and relative measurements of the concentration of PtdIns(3,4,5)P_3 and its different fatty-acyl species in small numbers of cells ($\geq 10^5$), either in suspension or adhered to tissue culture plates, and small samples of tissue.

Results

Establishing a quantitative assay for PtdIns(3,4,5)P_3

As part of our synthetic studies making phosphoinositides we observed that precursor compounds whose phosphates were protected with benzyl groups, in contrast to their de-protected forms, gave good ESI mass spectra. We therefore reasoned that chemically protecting the acidic phosphate groups of PtdIns(3,4,5)P_3 in biological extracts might offer a route to solving the major stability and sensitivity issues associated with its quantification by MS.

It was clear that the key to success would be the use of a mild and efficient method for the protection reaction. We chose to use trimethylsilyl diazomethane (TMS-diazomethane),

because it provides a relatively fast and clean method for the esterification of protonated phosphate groups at room temperature[15]. Further, the solvent mixture into which PtdIns(3,4,5)P_3 is extracted from cells most efficiently (a mixture of chloroform, methanol and H_2O with traces of HCl[16-17]) is an ideal environment for TMS-diazomethane reactions. Using TMS-diazomethane we were able to achieve rapid and complete methylation of the phosphate groups in PtdIns(3,4,5)P_3 with some mono-methylation of free hydroxyl groups in the inositol ring but no modification of unsaturated fatty acyl chains (see below). The methylated PtdIns(3,4,5)P_3 species were more efficiently transferred into the mass spectrometer, with a reduced number of ionic species, compared to their underivatised counterparts, both simplifying and effectively sensitizing the MS analysis.

We chromatographed derivatised lipid extracts through an in-line C4 column prior to infusion into a triple quadrapole mass spectrometer in the positive ion mode. This step concentrated the methylated PtdIns(3,4,5)P_3 species but co-elution with more abundant molecules necessitated a selective, second phase of mass fragmentation analysis (usually termed multiple reaction monitoring or MRM). Molecular ions selected in the first quadrapole were fragmented in the second quadrapole using collision parameters optimized for cleavage between the phosphoinositide headgroup and the glycerol unit, yielding a charged fragment corresponding to the diacylglycerol (DAG) and the neutral loss of a fragment corresponding to the methylated inositol phosphate headgroup (a neutral loss of 598amu for the major methylated species of PtdInsP_3; Supplementary Fig. 1). Since the mass of the charged DAG fragments can be determined and the products of further fragmentation can also be analyzed, then, in the context of previous work, it is possible to assign the likely structure of the DAGs and the parent lipids with some confidence. Further, whilst the focus of the study was on the measurement of PtdIns(3,4,5)P_3, the same principle of ‘measurement through neutral loss’ could be applied to the measurement of other lipids that fragmented similarly, for example measuring the DAG produced via loss of 490amu for the methylated headgroup of PtdInsP_2 or 213amu for the methylated headgroup of PtdSer, providing useful parallel data.

We first analyzed and quantified phosphoinositides in human neutrophils. Control or fMLP-stimulated human neutrophils were quenched with chloroform, methanol and HCl to create a single-phase extract into which non-biological C17:0/C16:0-PtdIns(3,4,5)P_3 was spiked as an internal standard (ISD). The samples were extracted, methylated and infused into the mass spectrometer. We initially performed neutral loss scans on parent ions whose masses were in a range consistent with either potential esterified PtdInsP_2 or PtdIns(3,4,5)P_3 species, with the detector set to measure daughter ions (putative DAGs) that were smaller by either 490 or 598amu (see Supplementary Table 1 for a list of relevant masses and associated structures). This revealed two relatively abundant species of PtdInsP_2 (m/z 1095 and 1117) in both control and stimulated cells (Fig. 1a,b) and two abundant species of PtdIns(3,4,5)P_3 (m/z 1203 and 1225) that were more concentrated in the stimulated cells (Fig. 1c,d). The daughter ions from neutrophil PtdInsP_2 with a parental m/z of 1117, and neutrophil PtdIns(3,4,5)P_3 with a parental m/z of 1225, created fragments identical to those derived from C18:0/C20:4-PtdIns(4,5)P_2 or –PtdIns(3,4,5)P_3 synthetic standards (Supplementary Figs. 2 and 3), strongly suggesting the biological phosphoinositides were both C18:0/C20:4, stearoyl/arachidonoyl species. The masses and further fragmentation of the additional PtdInsP_2 (m/z 1095) and PtdIns(3,4,5)P_3 (m/z 1203) species that we identified suggest they both contained C18:0/C18:1 (stearoyl/oleoyl) fatty acids (data not shown). We also detected other, lower abundance species but did not analyze them further.

The selectivity of the neutral loss transition is evident from comparing traces quantifying all ions derived from the neutrophil extract with an m/z of 1225 (Fig. 1e) to traces quantifying only those ions with an m/z of 1225 that underwent an m/z 1225 to m/z 627 + 598 transition

(Fig. 1f). The clarity with which fMLP increased the levels of the species quantified and the extent to which wortmannin, a selective PI3K inhibitor, prevented this increase provided biological confirmation that the assignment of ions to parental PtdIns(3,4,5)P_3 species was correct.

We refined our approach into a reliable and quantitative assay for targeted PtdIns(3,4,5)P_3 species. We found that synthetic ISD or C18:0/C20:4-PtdIns(3,4,5)P_3 that had been spiked into primary neutrophil extracts, esterified and processed for MS analysis was stable in mixtures of methanol/water (80%/20%) for ≥ 23h at room temperature (Fig. 2a,b) and could be detected in un-stimulated extracts when as little as 0.25ng had been added with excellent signal to noise (Fig. 2c). Further, both biological and synthetic PtdIns(3,4,5)P_3 species were routinely methylated to the same relative extent (Supplementary Fig. 4 and Supplementary Table 2) and were detected with linear efficiency and sensitivity over at least a 0.5-20ng range (Fig. 2d and Supplementary Fig. 5). If increasing amounts of synthetic C18:0/C20:4 PtdIns(4,5)P_2 were added to neutrophil extracts, it had no effect on the quantification of a parallel, internal spike of C18:0/C20:4-PtdIns(3,4,5)P_3 (Supplementary Fig. 6), showing the fidelity of the assay. If 10 ng ISD was spiked into primary extracts from different numbers of neutrophils then there was a reduction in both its, and the endogenous PtdInsP_2 and PtdIns(3,4,5)P_3's, recovery with increasing cell number (Supplementary Fig. 7). However, when the amount of the endogenous C18:0/C20:4-PtdInsP_2 or -PtdIns(3,4,5)P_3 detected in these samples was corrected for the recovery of the internal ISD, a linear relationship between endogenous PtdInsP_2 or PtdIns(3,4,5)P_3 and cell number was observed (Fig. 2e, parallel data for C18:0/C20:4-PtdInsP_2 are shown in Supplementary Fig. 7).

These results all indicate that through use of an internal, non-biological standard, C17:0/C16:0-PtdIns(3,4,5)P_3 (ISD), to correct for recovery through the extraction, methylation and mass spectrometry phases, this is a very sensitive and robust method to measure the relative levels of individual PtdIns(3,4,5)P_3 species in cells. Correction to the recovery of the ISD also proved to be a good normalization factor for other lipids measured in parallel, typically up to twenty three other lipids, including five different molecular species of PtdIns(3,4,5)P_3 and PtdInsP_2 from a single extract. We also noted that the ionizations of PtdIns(4,5)P_2 and PtdIns(3,4,5)P_3 in HPLC eluate were very similar, hence their ion currents were good indicators of their relative amounts (Fig. 2f). A completely confident measure of the absolute amounts of a particular molecular species however, requires the synthesis of the equivalent molecule to both calibrate the method and confirm the fragmentation analysis. This was only done for C18:0/C20:4-PtdIns(3,4,5)P_3 and C18:0/C20:4-PtdIns(4,5)P_2 in the current study.

Quantifying PtdIns(3,4,5)P_3 species in fMLP-stimulated human neutrophils

We used this approach to measure changes in PtdInsP_2 and PtdIns(3,4,5)P_3 molecular species in human neutrophils stimulated with fMLP, a setting where much previous work with other methods[18-21] has given a clear bench mark. We found that fMLP stimulated a small, transient and parallel reduction in the levels of both C18:0/C20:4- and C18:0/C18:1-PtdInsP_2 (Fig. 3a), that is known to result from activation of PLCβ[22], and a parallel increase in C18:0/C20:4- and C18:0/C18:1-PtdIns(3,4,5)P_3, that is known to result from activation of PI3Kγ[23-24] (Fig. 3b). The scale and kinetics of these responses were entirely in-keeping with earlier, quantitative data for total PtdIns(3,4,5)P_3 measured by competitive binding assay[18], 'fat-blot' assay[20] and metabolic labeling with either [^{3}H]-myo-inositol or [^{32}P]-Pi[19,21]. Further, our analysis accurately defines the basal as well as the stimulated levels of PtdIns(3,4,5)P_3 in 10^5 cells and, through calibration with synthetic C18:0/C20:4-PtdIns(3,4,5)P_3, absolute molar amounts of this species.

These results suggest that the two common species of $PtdInsP_2$ and $PtdIns(3,4,5)P_3$ that we detect in human neutrophils, of which the C18:0/C20:4-containing molecules are the most abundant, are both available and recognized by the relevant $PtdInsP_2$ and $PtdIns(3,4,5)P_3$ metabolising enzymes. However, a careful analysis of the conversion of each molecular species of $PtdInsP_2$ into its respective $PtdIns(3,4,5)P_3$ (Fig. 3c), indicated that C18:0/C20:4-$PtdIns(3,4,5)P_3$ accumulated selectively on fMLP-stimulation ($p<0.0001$, 2 way ANOVA, factors being species and time for 6-120 s).

Quantifying $PtdIns(3,4,5)P_3$ species in EGF-stimulated MCF10a cells

MCF10a cells are an immortalised human breast epithelial cell line that has been used to create a panel of homologously-targeted variants relevant to the study of PI3K signalling pathways[25-26], including deletion of the $PtdIns(3,4,5)P_3$ 3-phosphatase PTEN. These cells are highly adherent and hence we first adapted the extraction protocol to avoid the need for chloroform contact with the tissue culture plastic, then attempted to detect $PtdInsP_2$ and $PtdIns(3,4,5)P_3$ molecular species. Neutral loss scans revealed five common fatty-acyl species of both $PtdInsP_2$ and $PtdIns(3,4,5)P_3$ (Fig. 4a,b; these species were also detected in neutral loss scans of PtdInsP and PtdIns, data not shown). We quantified these five species in extracts from 10^5 growing, starved or starved then EGF-stimulated wild-type or $PTEN^{-/-}$ MCF10a cells (Fig. 4c,d). The efficiency of the extraction process was determined using an internal spike of ISD and variations in cell-input were corrected using the quantity of methylated C18:0/C18:1-PtdSer we recovered from the same extracts. In a small number of parallel assays we also quantified phosphoinositide pools in these cells using conventional ^{3}H-myo-inositol labeling and quantification of deacylated phosphoinositides by anion-exchange HPLC. The relative sizes of the total $PtdInsP_2$ and $PtdIns(3,4,5)P_3$ pools derived using either assay format were remarkably similar and exhibited similar changes upon EGF-stimulation (Supplementary Fig. 8), supporting the fidelity of the mass spectrometric analysis.

The concentrations of all five species of $PtdIns(3,4,5)P_3$ were increased by EGF-stimulation in a manner augmented by loss of PTEN (Fig. 4d). Interestingly, although C18:0/C20:4-$PtdInsP_2$ was the least abundant species of $PtdInsP_2$, this fatty-acyl species accumulated selectively in the $PtdIns(3,4,5)P_3$ pool upon EGF-stimulation (Fig. 4e; $p<0.0001$, 2 way ANOVA, factors being species and conditions).

Quantifying $PtdIns(3,4,5)P_3$ species in fat and liver

Quantification of $PtdIns(3,4,5)P_3$ in small samples of tissue remains an academically and commercially important challenge. We used our approach to measure Class I PI3K activity *in vivo* by studying the effects of insulin on mouse liver and human fat.

Mice of either wild-type or *Gnasxl*$^{m+/p-}$ genetic background (*Gnasxl*$^{m+/p-}$ mice lack XLαS, the imprinted isoform of Gαs, and are hyper-sensitive to insulin[27]) were injected intra peritoneal with insulin or a saline control and 8 minutes later samples of liver were frozen rapidly. Primary lipid extracts were spiked with ISD and then processed as described. Neutral loss scans revealed that C18:0/C20:4-molecular species were by far the most abundant versions of both $PtdInsP_2$ and $PtdIns(3,4,5)P_3$ in these samples (Fig. 5a and Supplementary Fig. 9). We then quantified C18:0/C20:4-$PtdIns(3,4,5)P_3$ and other phosphoinositides as described above using C18:0/C20:4-PtdSer to correct for sample size. In parallel, we prepared SDS lysates from the same frozen specimens to quantify phosphorylation of PKB, as a known marker of PI3K activation. Insulin stimulated a substantial increase in the levels of C18:0/C20:4-$PtdIns(3,4,5)P_3$ that was augmented in the *Gnasxl*$^{m+/p-}$ genetic background (Fig. 5b) but had no effect on the levels of C18:0/C20:4-$PtdInsP_2$ (Supplementary Fig. 9). Insulin also increased phosphorylation of PKB in the liver

samples, although this response appeared less strongly augmented in the Gnasxl$^{m+/p-}$ genetic background (Fig. 5c and Supplementary Fig. 10).

Human adipose tissue is highly responsive to changes in blood insulin. We starved healthy human volunteers overnight and removed and froze small biopsies of adipose tissue both before and 90 minutes after oral ingestion of glucose. We made a minor modification to our standard extraction procedure to pre-deplete the neutral storage lipids prior to extracting the polyphosphoinositides. This had no effect on recovery of ISD or endogenous PtdInsP_2 and PtdIns(3,4,5)P_3 species, but reduced recovery of less polar lipids such as PtdIns and PtdSer. Neutral loss scans revealed that the main molecular species of both PtdInsP_2 and PtdIns(3,4,5)P_3 was C18:0/C20:4 (Fig. 5d and Supplementary Fig.9). We quantified C18:0/C20:4-PtdIns(3,4,5)P_3 as above, but using PtdInsP_2 to correct for the amount of tissue (because recovery of PtdSer was poor under the modified conditions). In parallel, we prepared SDS lysates and quantified phosphorylation of PKB. These experiments showed the levels of C18:0/C20:4-PtdIns(3,4,5)P_3 were increased following ingestion of glucose (Fig. 5e) and this was paralleled by an increase in PKB phosphorylation (Fig. 5f and Supplementary Figs. 9 and 10).

Discussion

Since PtdIns(3,4,5)P_3 is the sole PtdInsP_3 in cells it can be quantified directly by our approach without the need for further purification from other regio-isomers prior to infusion into a mass spectrometer. In principle however, this approach could be extended to the quantification of other phosphoinositides if it could be coupled to a method that could distinguish between positional isomers on the inositol ring e.g. distinguishing between the three biological isomers of PtdInsP_2 (PtdIns(4,5)P_2, PtdIns(3,5)P_2 and PtdIns(3,4)P_2 or PtdInsP (PtdIns3P, PtdIns4P and PtdIns5P).

In addition to providing a sensitive and reproducible route to quantifying PtdIns(3,4,5)P_3 and related phosphoinositides, the methodology described here also identifies the fatty acyl complement of the molecular species measured. In all of the primary cells and tissues that we investigated, the most abundant species of PtdIns(3,4,5)P_3, PtdInsP_2, PtdInsP and PtdIns was, by far, the stearoyl/arachidonoyl form. This is consistent with much previous work indicating arachidonate is highly and selectively enriched in the *sn*-2 position of phosphoinositides[7,9,12]. The striking exception was MCF10a cells, where the stearoyl/arachidonoyl species of these lipids were amongst the least prevalent. Others have reported that cell lines grown in the presence of serum become “deficient” in arachidonate[28], potentially explaining this observation. Strikingly, however, the stearoyl/arachidonoyl form of PtdIns(3,4,5)P_3 selectively accumulated in both EGF-stimulated MCF10a cells and fMLP-stimulated neutrophils relative to its levels of enrichment in the total cell pool of its precursor, PtdInsP_2. This suggests mechanisms must exist to selectively accumulate the stearoyl/arachidonoyl form of PtdIns(3,4,5)P_3 in stimulated cells, raising important questions as to how this occurs and why.

Supplementary Material

Refer to Web version on PubMed Central for supplementary material.

Acknowledgments

We would like to thank G. Kelsey (Babraham Institute) for provision of mice and E. Ivanova for technical assistance. We also would like to thank A. Segonds-Pichon for statistical analysis. V. Juvin is a Marie Curie fellow. This work is supported by the Biotechnology and Biological Sciences Research Council and European Union FP7 LipidomicNet (#202272).

Online Methods

Materials

Trimethylsilyl diazomethane (TMS-diazomethane) as a 2 M solution in hexanes, was from Sigma-Aldrich Inc. Analytical grade formic acid, trifluoroacetic acid, and hydrochloric acid (HCl) were from Fisher Scientific Ltd. Chloroform (SpS grade, $CHCl_3$), methanol (SpS grade, MeOH), water (Ultra gradient grade, H_2O) and acetonitrile (Ultra gradient grade, ACN) were from Romil Ltd. 1-heptadecanoyl-2-hexadecanoyl-sn-glycero-3-(phosphoinositol-3,4,5-trisphosphate) (C17:0/C16:0-PtdIns(3,4,5)P_3, as a hepta-sodium salt) was used as an internal standard (ISD). The ISD was made at the Babraham Institute according to literature methods[29] and made up in a solution in water (0.1ng/μl). Synthetic C18:0/C20:4-PtdIns(3,4,5)P_3 and C18:0/C20:4-PtdIns(4,5)P_2 were from Avanti Polar Lipids. ^{3}H-inositol was from PerkinElmer. All cell culture reagents were from Invitrogen unless specified. All other reagents, unless specified, were from Sigma. All lipid extractions used 2 ml polypropylene safe-lock tubes (Eppendorf).

Stock solutions for lipid extractions

Prior to extraction, the following solutions were prepared using standard glassware; the quench mixture comprising of MeOH (484 ml), $CHCl_3$ (242 ml), and 1 M HCl (23.55 ml); the pre-derivisation wash composed of $CHCl_3$ (240 ml), MeOH (120 ml) and 0.01 M HCl (90 ml); and the post-derivatisation wash made up of $CHCl_3$ (240 ml), MeOH (120 ml), and H_2O (90 ml). Wash mixtures were shaken and allowed to separate into 2 phases. The top phase of each solution was used.

Preparation of Human Neutrophils

We isolated human neutrophils from the peripheral blood of healthy volunteers with written consent (REC Approval number 06/Q0108/165) as described previously[30]. Purity was determined by cytospin and REASTAIN Quick-Diff (Reagena) staining, and was at least 95%. After washing, we resuspended neutrophils in Dulbecco's PBS with Ca^{2+} and Mg^{2+}, glucose (1g l^{-1}), sodium bicarbonate (4 mM, DPBS+) at 3×10^7 ml^{-1}. Where appropriate, we stimulated aliquots (170 μl) of cells with fMLP (100 nM) for indicated times at 37 °C, and terminated reactions by addition of quench mix (750 μl), and extracted and processed lipids as described below. Where appropriate, we pre-treated cells with 300 nM of the PI3K inhibitor wortmannin for 10 min at 37 °C, prior to stimulation.

Preparation of MCF10a Cells

MCF10a PTEN$^{+/+}$ and PTEN$^{-/-}$ were provided by Horizon Discovery (Cambridge, UK) and maintained at 37 °C, 5% CO_2, in DMEM/F12 media (Invitrogen 31330), supplemented with horse serum (5%, PAA), hydrocortisone (0.5 μg ml^{-1}), insulin (10 μg ml^{-1}), cholera toxin (0.1 μg ml^{-1}) and EGF (2 ng ml^{-1}). When required, we starved cells in DMEM/F12 media supplemented with charcoal-stripped horse serum (1%, PAA) hydrocortisone and cholera toxin. Early passages of cells were used (13-15). We plated 2×10^5 cells onto tissue culture dishes (3.5 cms diameter) for 24 hr. Where indicated, we then starved cells for a further 16 hrs. We stimulated cells with EGF (2 ng ml^{-1}) for 15 min at 37 °C. Media was rapidly aspirated and 1 M HCl (0.5 ml, 4 °C) was added. We scraped cells from the plates and collected them. We spun cells (15000g, 5 min, 4 °C) and removed supernatants. We then resuspended the pellets in H_2O (170 μl) and quench mix (750 μl), and commenced extraction as described below.

For ^{3}H-inositol-labelling experiments, we starved cells in inositol-free DMEM/F12 (Millipore) containing dialysed bovine serum (1%, Sigma), hydrocortisone and cholera toxin, and supplemented with 100 μCi ml^{-1} ^{3}H-inositol (or equivalent amounts of myo-inositol for parallel, non-labelled experiments, 4.6 μM final concentration in the medium). We starved cells for 17 hrs, and then stimulated them with 2 ng ml^{-1} EGF for 2 min at 37 °C. Both ^{3}H-inositol labelled and unlabelled cells were processed as described above, and extracted identically to the point prior to derivatisation, where labelled cells were deacylated, extracted and separated by HPLC as described previously[6].

Preparation of Liver Samples

All animals were housed in the small animal barrier unit (SABU) at the Babraham Institute under specific pathogen-free conditions. We injected WT and *Gnasxl*$^{m+/p-}$ mice[27] that had been fasted overnight (16 hr), intraperitonally (I.P.) with saline or insulin (10 U kg^{-1} body weight). We collected livers 8 min after injection, rinsed them rapidly in cold PBS, and immediately froze them in liquid N_2. Frozen livers were stored at −80 °C until use. This work was performed on Home Office Project License PPL 80/2364.

For lipid extraction, we homogenised portions of frozen liver (3-4 mg) in a Dounce homogeniser with quench mix (1 ml). We collected the homogenate, then added a further aliquot of quench mix (1 ml) to the homogeniser and, after rinsing, this was removed and pooled with the first homogenate (total 2 ml). We diluted the final combined homogenates 1:5 with quench mix, and two aliquots (750 μl) were taken. We added H_2O (170 μl) to each aliquot, and then we extracted and processed these samples in parallel, as described below.

Preparation of Adipose Samples

Healthy human volunteers (from whom informed written consent was obtained) were fasted overnight, and needle biopsies of abdominal, subcutaneous, adipose tissue were taken after infiltrating the tissue with 1% lignocaine. We took biopsies before and 90 mins after oral ingestion of 75 g of glucose. We immediately rinsed biopsies in saline, then snap froze them in liquid N_2. For analysis we ground the frozen adipose to a fine powder with a mortar and pestle under liquid N_2. We homogenised aliquots of the frozen material (approximately 15 mg) in a Dounce homogeniser with $CHCl_3$/methanol (1:2, v:v, 1 ml) and washed through with a further wash (1 ml). Duplicate aliquots (725 μl) underwent additional processing, prior to standard extraction and processing of polar lipids, to remove neutral lipids, as described below.

Lipid extraction

We created primary lipid extracts from neutrophils, MCF10a cells, or liver samples, as described above. This resulted in a thoroughly mixed, single phase sample (from 170 μl of aqueous sample and 750 μl of quench mix) in a safe-lock polypropylene tube (2 ml). We then added an aliquot of ISD (10 μL containing 1 ng), vortexed and allowed the sample to stand for a further 5 min (RT). We then added $CHCl_3$ (725 μl) and 2 M HCl (170 μl), mixed the sample thoroughly again and centrifuged in a bench top microfuge (5000 rpm, 5 min, RT). This created a two-phase system with an upper aqueous layer and a protein band at the interface. We collected the lower organic phase into a fresh tube and then added pre-derivatisation wash (708 μl). We then vortexed briefly, centrifuged in a microfuge (5000 rpm, 3 min, RT) and collected the lower phase into another fresh tube for derivatisation (see below).

We removed neutral lipids from adipose homogenates by first adding H_2O (170 μl) and 50 mM LiOH (25 μl) to a 725 μl aliquot of adipose homogenate in $CHCl_3$/MeOH (1:2, v:v) and then mixing the sample thoroughly. We added 1 ng ISD, mixed and then added $CHCl_3$ (725 μl). We mixed the sample again, centrifuged (5000 rpm, 5 min, RT), and then removed the resultant lower phase (containing neutral lipids). We repeated the $CHCl_3$ wash step, and then added $CHCl_3$/methanol (500 μl, 2:1, v/v), 2 M HCl (170 μl), and $CHCl_3$ (500 μl) to the retained upper phase, vortexed thoroughly and then allowed the sample to stand for 5 min (RT). We centrifuged the sample (5000 rpm, 5 min, RT) and then collected the lower organic phase into a fresh tube. We added pre-derivatisation wash (708 μl), mixed and centrifuged to separate the phases. We then collected the resultant lower phase into a fresh tube prior to derivatisation.

Derivatisation

NOTE: Trimethylsilyl diazomethane (IUPAC name (Diazomethyl)trimethylsilane; abbreviated here TMS-diazomethane) is toxic by inhalation, producing central nervous system depression, drowsiness, dizziness and lung damage. Although it is not currently considered an explosive risk, and it is certainly less dangerous from this perspective than diazomethane, the authors would still advocate taking appropriate precautions and treat it as though it is. We routinely destroy excess reagent with care in 10% acetic acid in methanol solutions and rinse and immerse all syringes and glassware that might contain TMS-diazomethane in this solution. Be aware that when TMS-diazomethane is neutralised with acetic acid, nitrogen gas is evolved and it is a violent reaction, so if large volumes are being destroyed great care should be exercised. We advocate only using this reagent in a fume hood with adequate personal safety equipment, and that only people who have read the manufacturers safety data sheets and fully understand the risks carry this reaction out. We always do this reaction in the presence of a qualified chemist who can ensure that all appropriate safety measures are taken.

We added 2 M TMS-diazomethane in hexane (50 μl) to lipid extracts prepared as described above (approx I ml of ‘lower phase’), to give a yellow solution, and then allowed the reaction to proceed for 10 min, RT. We quenched reactions with glacial acetic acid (6μl), which removed the sample’s yellow colour (this reaction releases N_2 gas, thus care should be taken). We added post-derivatisation wash solution (700 μl) to the organic solution, and mixed the samples, which we then centrifuged (5000 rpm, 3 min), and collected the resultant lower phase. We repeated the wash step, and then added MeOH:H_2O (9:1 v:v, 100 μl) to the final collected lower phase. We dried samples under a stream of N_2 at RT until almost dry (about 10 μl remaining). We immediately dissolved samples in MeOH (80 μl), sonicated briefly, and added H_2O (20 μl). We subjected final samples to mass spectrometer analysis as described below.

Mass Spectrometer Analysis

Analysis of lipid profiles from neutrophil extracts (Figures 1a-d, 2a-e, and 3; and Supplementary Figures S2e and f, S3e and f, and S5-7) was performed on a Quattro Ultima mass spectrometer (Waters), connected to a Waters 2795 HPLC system. 90 μl sample injections were used. A 67% to 90% acetonitrile in water gradient over 20 minutes containing 0.1% trifluoroacetic acid (TFA) was used for separation on a 1 mm × 50 mm Jupiter C4 column from Phenomenex. Full details of these and other parameters for the Quattro Ultima mass spectrometer can be found in Supplementary data 1.

All other samples (Figures 1e and f, 2f, 5 and 6; and Supplementary Figures S2a-d, S3a-d, S4 and S8) were analysed using a ABSciex QTRAP 4000 connected to a Waters Acquity

Europe PMC Funders Author Manuscripts

UPLC system, with duplicate 45 μl samples injected. A 45% to 100% acetonitrile in water gradient over 15 minutes containing 0.1% formic acid was used with a Waters Acquity UPLC BEH 300 C4 1.7 μm, 1.0 × 100 mm column. Full details of these and other parameters for the QTRAP mass spectrometer can be found in Supplementary data 2.

Integrated area of lipid species peaks were corrected for recovery against ISD area (giving a response ratio for each lipid) and then, to account for cell number, normalised to PtdSer, also corrected to internal standard (C18:0/C20:4 PtdSer for liver, C18:0/C18:1 PtdSer for MCF10a cells - response ratios were found to be linear with cell number).

Phospho-PKB Western blot analysis

We resuspended frozen liver (50 mg) or adipose (5 mg) samples, that had been crushed to a fine powder in a mortar and pestle, in cold lysis buffer (20 mM Tris, pH 7.5, 150 mM NaCl, 1 mM EDTA, 1 mM EGTA, 0.1% Triton supplemented with 2.5 mM sodium pyrophosphate, 5 mM β-glycerol phosphate, 1 mM sodium orthovanadate, 1 mM sodium fluoride, 0.1 mM PMSF, and 10 μg ml-1 of anti-proteases leupeptin, aprotinin, antipain and pepstatin A). We allowed samples to lyse for 30 min, 4 °C with end-on-end rotation. We removed insoluble material by centrifugation (15000 g, 15 min, 4 °C), and quantified protein in the resultant supernatant by Bradford Protein Assay (Bio-Rad), before diluting in SDS-sample buffer. We separated proteins from 50 μg (liver) or 7.5 μg (adipose) samples by SDS-PAGE and transferred to PVDF membrane. We blotted samples for phosphoPKB and loading controls (actin, β-COP), using primary antibodies against phosphoPKB ser473(DE9) (Rabbit, Cell Signalling 4060, 1:2000), actin (Sigma A3853, mouse, 1:10,000), and β-COP (A kind gift from Nick Ktistakis, Babraham Institute, mouse, 1:200) in TBS/0.1% Tween, 5% BSA, 2 hr, RT; and secondary IgG antibodies InfraRedDye 680 Goat α-rabbit (926-32221, LI-COR), and 800CW Goat α-mouse (926-32210 LI-COR), 1:10,000 for 1 hr in the dark. Fluorescence was detected and quantitated with an Odyssey Imaging System (LI-COR), with Phospho-PKB signal corrected for loading controls.

Statistics

A 2-way ANOVA was used to analyse the data shown in Fig 3. The factors we isolated were time and species and we analysed all of the data except that for the un-stimulated (t= 0) controls. A 2-way ANOVA was used to analyse the data presented in Fig 4. The factors we isolated were the different molecular species and the conditions (i.e. WT, PTEN$^{-/-}$, growth medium, starved, EGF stimulated). We looked for differences between log2 ratios among species taking into account the different conditions. The “species effect” was significant ($p< 0.0001$) and hence we ran a post-hoc test (Dunnett’s pairwise multiple comparison t test) to compare the C18:0/C20:4 species against all others. All comparisons were highly significant ($p< 0.0001$).

References

1. Cantley LC. The phosphoinositide 3-kinase pathway. Science. 2002; 296:1655–1657. [PubMed: 12040186]
2. Vanhaesebroeck B, et al. Synthesis and function of 3-phosphorylated inositol lipids. Annu Rev Biochem. 2001; 70:535–602. [PubMed: 11395417]
3. Vanhaesebroeck B, Vogt PK, Rommel C. PI3K: From the Bench to the Clinic and Back. Curr Top Microbiol Immunol. 2010; 347:1–19. [PubMed: 20549473]
4. Rusten TE, Stenmark H. Analyzing phosphoinositides and their interacting proteins. Nat Methods. 2006; 3:251–258. [PubMed: 16554828]

5. Sauer K, Huang YH, Lin H, Sandberg M, Mayr GW. Phosphoinositide and inositol phosphate analysis in lymphocyte activation. Curr Protoc Immunol. 2009; 87:11.1.1–11.1.46.
6. Guillou H, Stephens LR, Hawkins PT. Quantitative measurement of phosphatidylinositol 3,4,5-trisphosphate. Methods Enzymol. 2007; 434:117–130. [PubMed: 17954245]
7. Milne SB, Ivanova PT, DeCamp D, Hsueh RC, Brown HA. A targeted mass spectrometric analysis of phosphatidylinositol phosphate species. J Lipid Res. 2005; 46:1796–1802. [PubMed: 15897608]
8. Wenk MR, et al. Phosphoinositide profiling in complex lipid mixtures using electrospray ionization mass spectrometry. Nat Biotechnol. 2003; 21:813–817. [PubMed: 12808461]
9. Pettitt TR, Dove SK, Lubben A, Calaminus SD, Wakelam MJ. Analysis of intact phosphoinositides in biological samples. J Lipid Res. 2006; 47:1588–1596. [PubMed: 16632799]
10. Ivanova PT, Milne SB, Myers DS, Brown HA. Lipidomics: a mass spectrometry based systems level analysis of cellular lipids. Curr Opin Chem Biol. 2009; 13:526–531. [PubMed: 19744877]
11. Postle AD, Wilton DC, Hunt AN, Attard GS. Probing phospholipid dynamics by electrospray ionisation mass spectrometry. Prog Lipid Res. 2007; 46:200–224. [PubMed: 17540449]
12. Vadnal RE, Parthasarathy R. The identification of a novel inositol lipid, phosphatidylinositol trisphosphate (PIP3), in rat cerebrum using in vivo techniques. Biochem Biophys Res Commun. 1989; 163:995–1001. [PubMed: 2551281]
13. Ogiso H, Taguchi R. Reversed-phase LC/MS method for polyphosphoinositide analyses: changes in molecular species levels during epidermal growth factor activation in A431 cells. Anal Chem. 2008; 80:9226–9232. [PubMed: 19551943]
14. Vasudevan KM, et al. AKT-independent signalling downstream of oncogenenic PIK3CA mutations in human cancer. Cancer Cell. 2009; 16:21–32. [PubMed: 19573809]
15. Oku N, et al. Isolation, structural elucidation, and absolute stereochemistry of enigmazole A, a cytotoxic phosphomacrolide from the Papua New Guinea marine sponge Cinachyrella enigmatica. J Am Chem Soc. 2010; 132:10278–10285. [PubMed: 20590096]
16. Corey S, et al. Granulocyte macrophage-colony stimulating factor stimulates both association and activation of phosphoinositide 3OH-kinase and src-related tyrosine kinase(s) in human myeloid derived cells. Embo J. 1993; 12:2681–2690. [PubMed: 8392933]
17. Folch J, Lees M, Sloane Stanley GH. A simple method for the isolation and purification of total lipides from animal tissues. J Biol Chem. 1957; 226:497–509. [PubMed: 13428781]
18. Cadwallader KA, et al. Regulation of phosphatidylinositol 3-kinase activity and phosphatidylinositol 3,4,5-trisphosphate accumulation by neutrophil priming agents. J Immunol. 2002; 169:3336–3344. [PubMed: 12218155]
19. Traynor-Kaplan AE, Harris AL, Thompson BL, Taylor P, Sklar LA. An inositol tetrakisphosphate-containing phospholipid in activated neutrophils. Nature. 1988; 334:353–356. [PubMed: 3393226]
20. Guillou H, et al. Use of the GRP1 PH domain as a tool to measure the relative levels of PtdIns(3,4,5)P3 through a protein-lipid overlay approach. J Lipid Res. 2007; 48:726–732. [PubMed: 17130283]
21. Stephens LR, Hughes KT, Irvine RF. Pathway of phosphatidylinositol(3,4,5)-trisphosphate synthesis in activated neutrophils. Nature. 1991; 351:33–39. [PubMed: 1851250]
22. Li Z, et al. Roles of PLC-beta2 and -beta3 and PI3Kgamma in chemoattractant-mediated signal transduction. Science. 2000; 287:1046–1049. [PubMed: 10669417]
23. Condliffe AM, et al. Sequential activation of class IB and class IA PI3K is important for the primed respiratory burst of human but not murine neutrophils. Blood. 2005; 106:1432–1440. [PubMed: 15878979]
24. Van Keymeulen A, et al. To stabilize neutrophil polarity, PIP3 and Cdc42 augment RhoA activity at the back as well as signals at the front. J Cell Biol. 2006; 174:437–445. [PubMed: 16864657]
25. Gustin JP, et al. Knockin of mutant PIK3CA activates multiple oncogenic pathways. Proc Natl Acad Sci U S A. 2009; 106:2835–2840. [PubMed: 19196980]
26. Vitolo MI, et al. Deletion of PTEN promotes tumorigenic signaling, resistance to anoikis, and altered response to chemotherapeutic agents in human mammary epithelial cells. Cancer Res. 2009; 69:8275–8283. [PubMed: 19843859]

27. Xie T, et al. The alternative stimulatory G protein alpha-subunit XLalphas is a critical regulator of energy and glucose metabolism and sympathetic nerve activity in adult mice. J Biol Chem. 2006; 281:18989–18999. [PubMed: 16672216]

28. Rouzer CA, et al. Lipid profiling reveals arachidonate deficiency in RAW264.7 cells: Structural and functional implications. Biochemistry. 2006; 45:14795–14808. [PubMed: 17144673]

29. Painter GF, et al. General synthesis of 3-phosphorylated myo-inositol phospholipids and derivatives. Journal of the Chemical Society-Perkin Transactions 1. 1999; (8):923–935.

30. Anderson KE, et al. CD18-dependent activation of the neutrophil NADPH oxidase during phagocytosis of Escherichia coli or Staphylococcus aureus is regulated by class III but not class I or II PI3Ks. Blood. 2008; 112:5202–5211. [PubMed: 18755982]

Europe PMC Funders Author Manuscripts

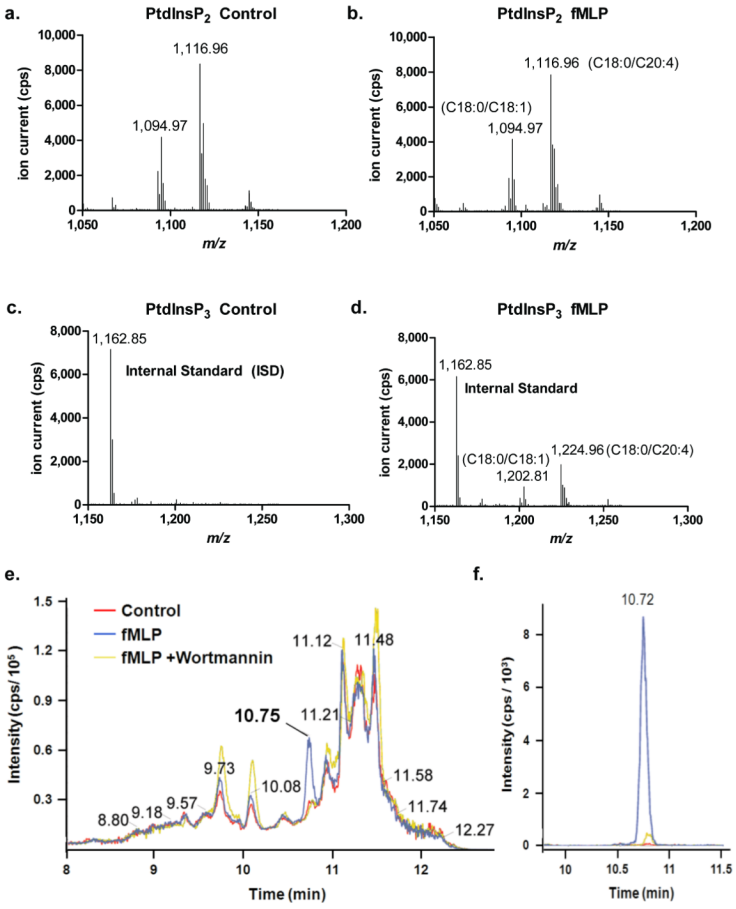

Figure 1.

Analysis of phosphoinositides in control and fMLP-stimulated human neutrophils. (**a-d**) Neutral loss scans of a derivatised phosphoinositide extract, from un-stimulated control (**a**, **c**) or fMLP-stimulated (**b**, **d**) neutrophils, ISD = internal standard. The two most abundant species of endogenous PtdIns(3,4,5)P_3 and PtdInsP_2 are labeled with full masses and corresponding fatty acid species of DAG unit. (**e**) Overlay of m/z chromatograms for parent ions with masses similar to derivatised C18:0/C20:4-Ptdins(3,4,5)P_3 from extracts from 1 $\times 10^5$ human neutrophils, highlighting elution at 10.75 min (ions which increase with fMLP-stimulation in a wortmannin-sensitive manner). (**f**) Overlay of MRM chromatograms (m/z 1,225 → m/z 627 + 598) of samples from **e**. Data in **a-d** were collected using a Quattro Ultima mass spectrometer and data in **e-f** were collected using a QTRAP4000 mass spectrometer. Each are representative traces from several independent experiments. A full list of relevant structures and associated masses are shown in Supplementary Table 1; *sn*-1/*sn*-2 assignment is based on biological precedent and further fragmentation of DAG species.

Europe PMC Funders Author Manuscripts

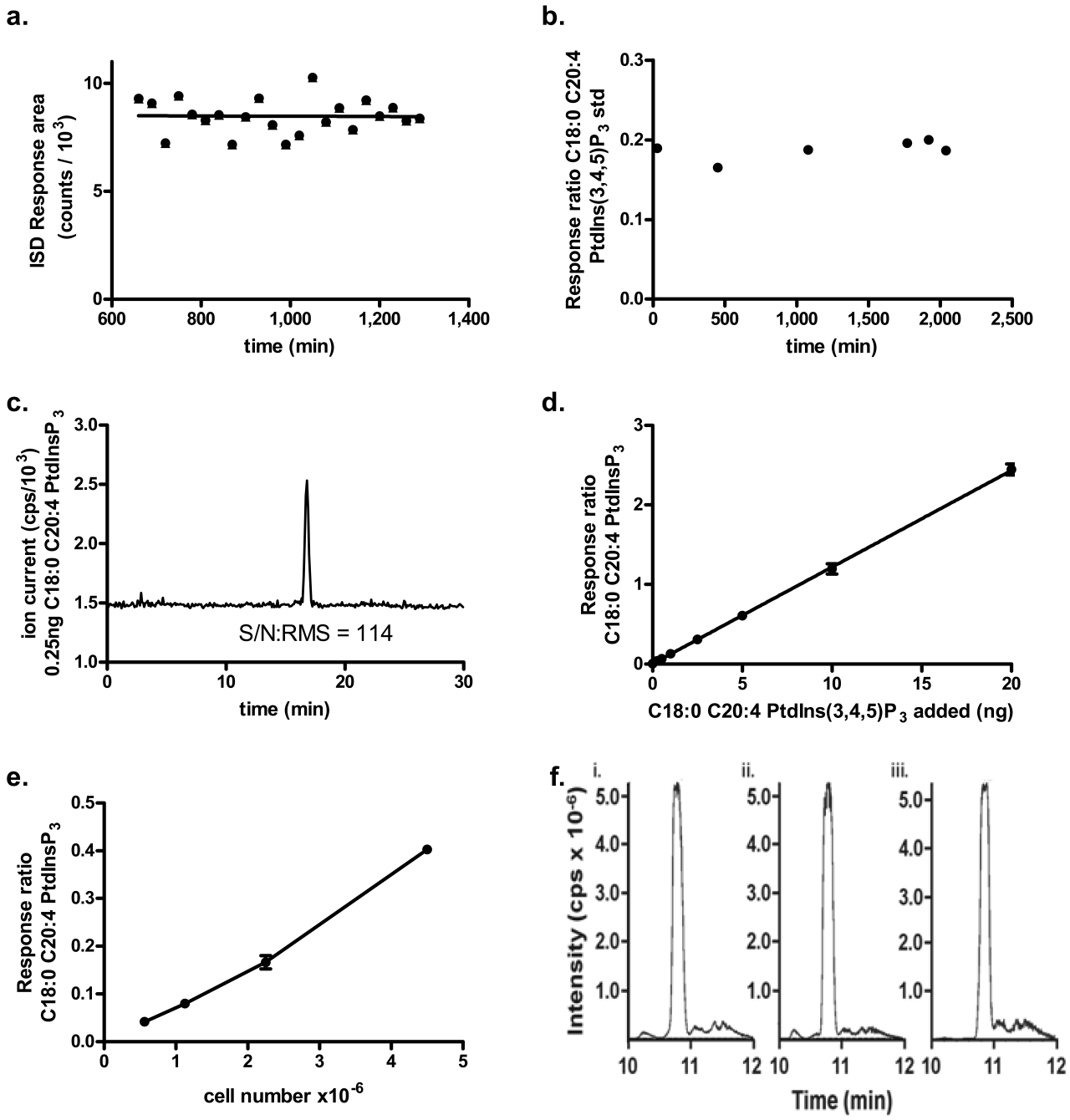

Figure 2.

Validation of the robustness, signal-to-noise and linearity of the assay. **a**) C17:0/C16:0-PtdIns(3,4,5)P_3 internal standard (ISD) spiked into un-stimulated human neutrophil extract; (**b**) C18:0/C20:4-PtdIns(3,4,5)P_3 standard spiked into un-stimulated human neutrophil extract; (**c**) 0.25 ng C18:0/C20:4-PtdIns(3,4,5)P_3 standard spiked into un-stimulated neutrophil extract; (**d**) linear response to increasing amounts of C18:0/C20:4-PtdIns(3,4,5)P_3 added to extracts of un-stimulated neutrophils (2.25×10^6); (**e**) linear relationship between cell number (fMLP-stimulated neutrophils) and estimated endogenous C18:0/C20:4-PtdIns(3,4,5)P_3 by using the ISD to correct for recovery. The term 'response ratio' in (**b,d,e)**

is the integrated ion current response to the defined phosphoinositide divided by that to the ISD. (**f**) MRM chromatograms for 1μg each of synthetic C18:0/C20:4-PtdIns(4,5)P_2 (**i**), synthetic C18:0/C20:4-PtdIns(3,4,5)P_3 (**ii**) and ISD (C17:0/C16:0-PtdIns(3,4,5)P_3) (**iii**) in water, demonstrating equal recovery/detection.

Europe PMC Funders Author Manuscripts

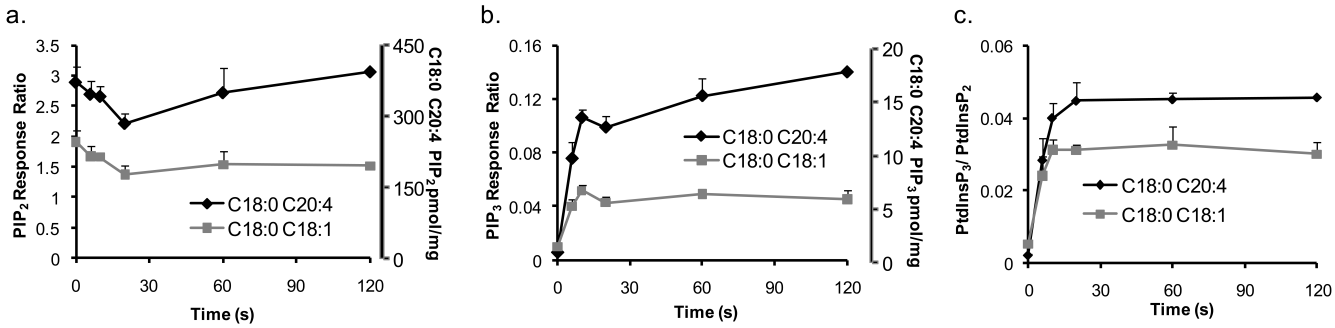

Figure 3.

fMLP-stimulated changes in C18:0/C20:4 and C18:0/C18:1 PtdInsP_2 and PtdIns(3,4,5)P_3 species in human neutrophils. (**a-b**) The levels of the C18:0/C20:4 and C18:0/C18:1 molecular species of PtdInsP_2 (**a**) and PtdIns(3,4,5)P_3 (**b**) in human neutrophils were determined at a range of times following addition of fMLP. The data are expressed as either response ratios (as defined in fig. 2) or, through use of the calibration curve presented in Fig. 2d, and protein assays, pmol mg^{-1} protein (Y-axis, right) and are means ± SEM (n= 4). (**c**) The ratio of the quantity of each molecular species of PtdIns(3,4,5)P_3 divided by that of their respective PtdInsP_2 species.

Europe PMC Funders Author Manuscripts

Europe PMC Funders Author Manuscripts

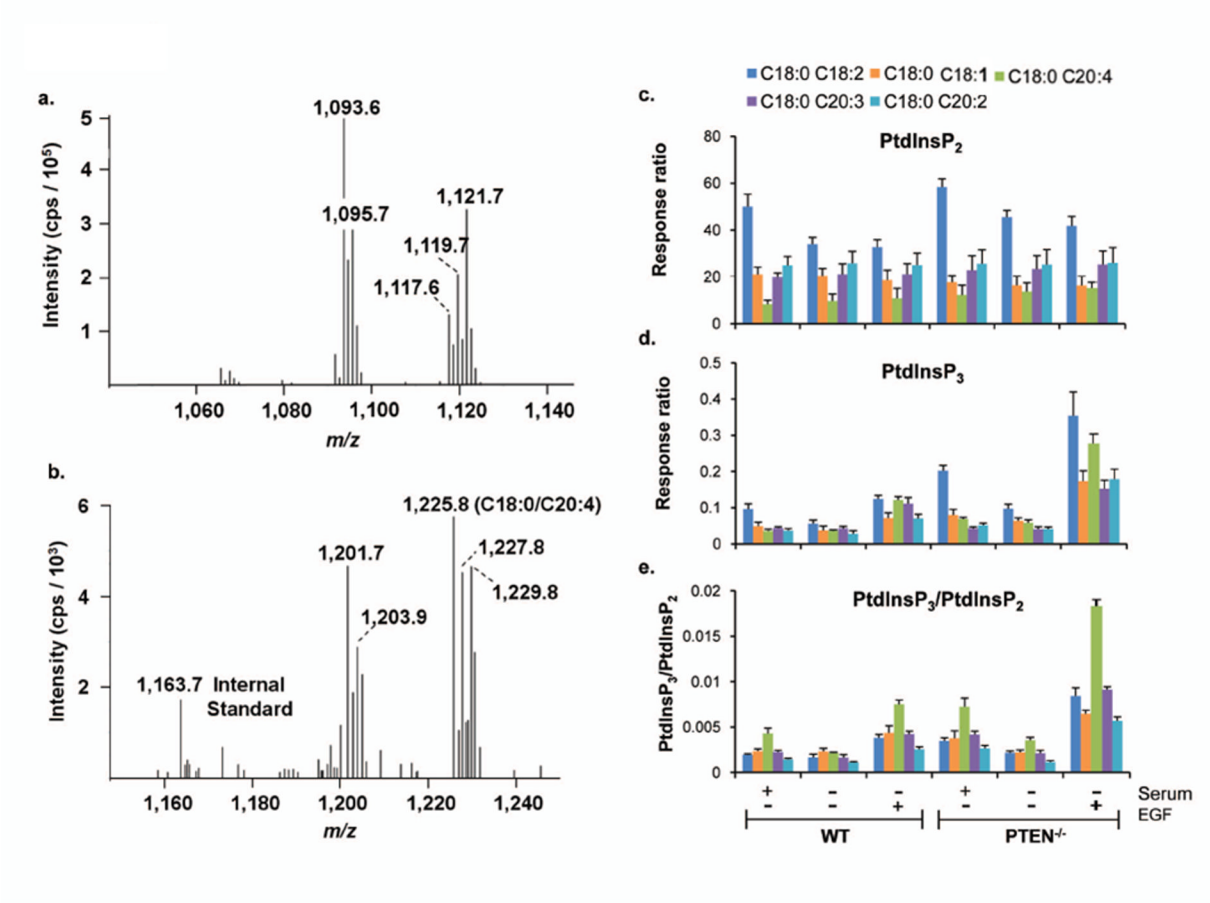

Figure 4.

Identification and quantification of the molecular species of PtdIns(3,4,5)P_3 in wild-type and PTEN$^{-/-}$ MCF10a cells. (**a-b**) Neutral loss scans of the common families of molecular species of PtdInsP_2 (**a**) and PtdIns(3,4,5)P_3 (**b**) in EGF-stimulated, wild-type MCF10a cells, Further fragmentation and analysis of the relevant daughter ions indicated they possessed the fatty acids indicated in **c,d**. Data was collected using a QTRAP 4000 mass spectrometer. (**c-d**) The levels of these species of PtdInsP_2 (**c**) and PtdIns(3,4,5)P_3 (**d**) in the indicated cell lines and conditions are presented as mean response ratios normalized for cell input via the recovered C18:0/C18:1-PtdSer (means ± SEM, n= 3). (**e**) The ratio of the quantity of each molecular species of PtdIns(3,4,5)P_3 divided by that of their respective PtdInsP_2 species. Full details of molecular species, and masses of respective parent ions detected in MCF10a cells can be found in Supplementary Table 1.

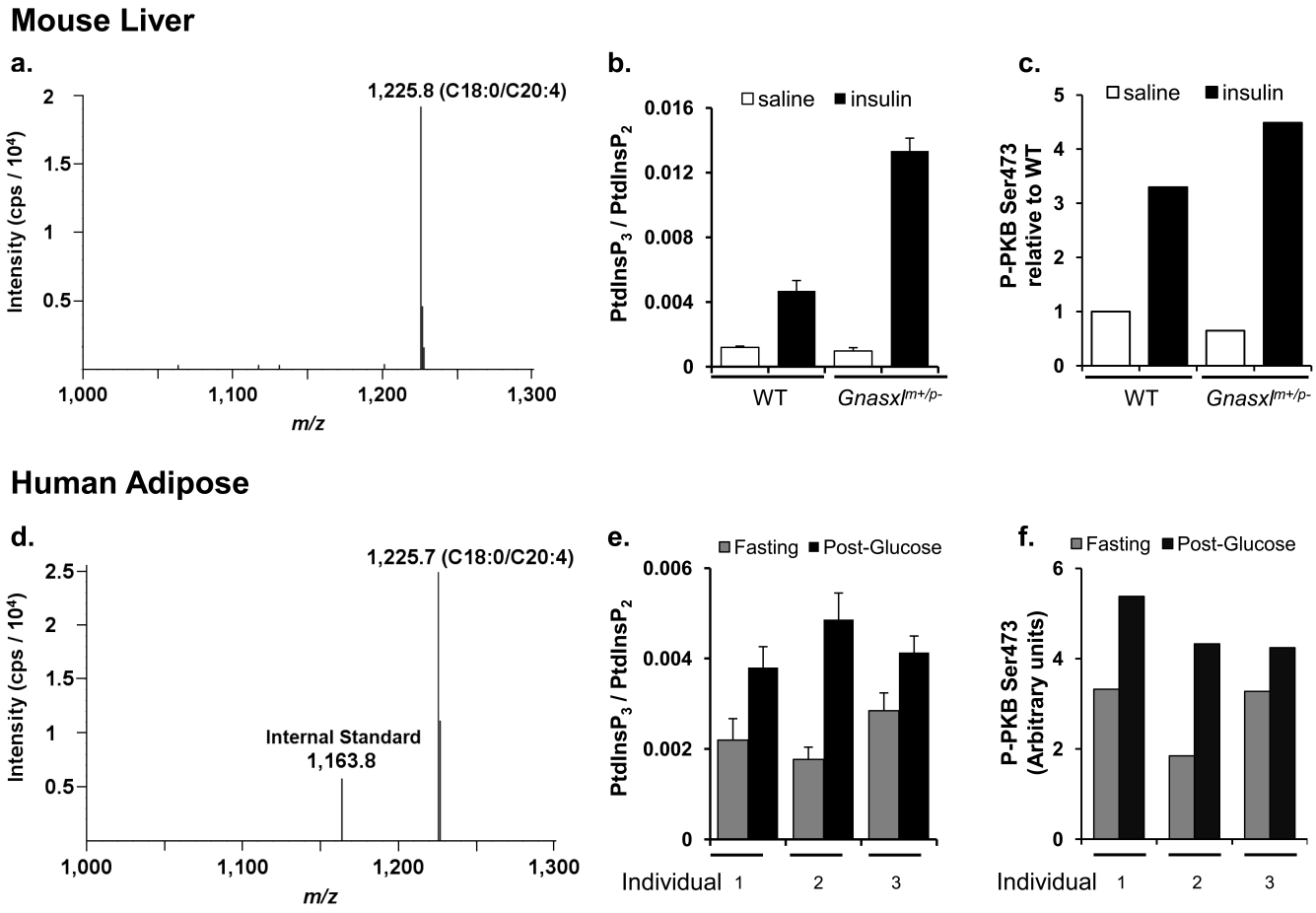

Figure 5.

Detection and quantification of insulin-stimulated PtdIns(3,4,5)P_3 responses in mouse liver and human adipose tissue. (**a**) Neutral loss scan, collected using a QTRAP 4000 mass spectrometer, of PtdIns(3,4,5)P_3 species in wild-type (WT), insulin-stimulated mouse liver. (**b**) Levels of C18:0/C20:4-PtdIns(3,4,5)P_3 in the livers of WT or *Gnasxl*$^{m+/p-}$ mice, after injection of insulin or saline (means ± SEM, n= 4). (**c**) Phosphorylation status of S473 in PKB for parallel samples to those analyzed in **b**; data normalized for input material *via* immuno-blotting for β-COP (See Supplementary Fig. 10 for blot). (**d**) Neutral loss scan of PtdIns(3,4,5)P_3 species in human adipose tissue following oral ingestion of glucose. (**e**) Levels of C18:0/C20:4-PtdIns(3,4,5)P_3 in healthy human adipose tissue following overnight starvation either before (Fasting) or 90 mins after (Post-Glucose) oral ingestion of glucose, for three individuals (means ± SEM, technical replicates n= 4). (**f**) Phosphorylation status of S473 in PKB for parallel samples to those analyzed in **e**; data normalized for input material *via* immuno-blotting for actin (See Supplementary Fig. 10 for blot).